Available online at www.sciencedirect.com

ScienceDirect

Mendeleev Commun., 2018, **28**, 447–449

Mendeleev Communications

The modes of combustion of copper nanopowders

Michail I. Alymov,[a] Nikolai M. Rubtsov,*[a] Boris S. Seplyarskii,[a] Victor A. Zelensky,[a] Alexey B. Ankudinov,[b] Georgii I. Tsvetkov[a] and Victor I. Chernysh[a]

[a] *Institute of Structural Macrokinetics and Materials Science, Russian Academy of Sciences, 142432 Chernogolovka, Moscow Region, Russian Federation. Fax: +7 495 962 8025; e-mail: nmrubtss@mail.ru*

[b] *A. A. Baikov Institute of Metallurgy and Materials Science, Russian Academy of Sciences, 119991 Moscow, Russian Federation*

DOI: 10.1016/j.mencom.2018.07.037

It was shown that the synthesis of Cu nanopowder by thermal decomposition afforded chemically purer (without oxides) and finer (specific surface value ~45 m^2 g^{-1}) product than the synthesis by chemical reduction. The latter method leads to pyrophoric nanopowders containing detectable amounts of copper oxides.

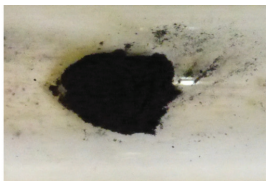

Nanomaterials are applied in diverse fields of engineering and technology.[1–4] One of the key benefits of nanomaterials is that their properties differ from those of bulk material of the same composition. For example, the properties of nanoparticles may be easily altered by varying their size, shape, and chemical environment. Copper is found to be too soft for some applications, and hence it is often combined with other metals to form numerous alloys such as brass, which is a copper–zinc alloy. Copper nanoparticles are graded as highly flammable solids and must be stored away from sources of ignition. However, little is known about the combustibility of Cu nanopowders.

Among various metal nanoparticles, Cu nanoparticles have been paid much attention in recent years because of their intrinsic properties and wide potential applications in many fields such as photochemical catalysis, bio, gas and electrochemical sensing, and solar/photovoltaic energy conversion.[2–4] The key applications of copper nanoparticles are as follows: (1) an anti-biotic, anti-microbial, and anti-fungal agent added to plastics, coatings, and textiles;[5,6] (2) a component of high strength metals and alloys, heat sinks and highly thermal conductive materials; (3) an efficient catalyst for chemical reactions, *e.g.* for the synthesis of methanol and glycol; (4) a constituent in sintering additives and capacitor materials.[7] In addition, conductive inks and pastes containing Cu nanoparticles may be used as a substitute for very expensive noble metals in printed electronics, displays, and conductive thin film applications, as well as for the processing of superficial conductive coatings for metal surfaces and nanometal lubricant additives.[7]

The synthesis of Cu nanoparticles is processed *via* various routes, *viz.*, chemical reduction,[8] thermal decomposition,[9] the polyol method,[10] reverse micelles,[11] electron beam irradiation,[12] micro-emulsion techniques,[13] wire explosion[14] and *in situ* chemical synthesis.[15]

As mentioned above, copper nanoparticles can be flammable. To make possible the processing in ambient air, the nanopowders must be either stored under inert liquid or protected. The protection (passivation) means the obtaining of thin oxide films on the surface of nanoparticles, which prevents the oxidation and provides preservation of their unique properties.[16,17]

The objective of the present investigation was the establishment of thermal combustion modes of Cu nanoparticles obtained both by the method of chemical metallurgy and thermal decomposition of copper salts as well as the conditions of their passivation. In addition, partial characterization of the synthesized Cu nanopowders was performed.

For experimental studies of the ignition processes, we used Cu nanopowders obtained by the method of chemical metallurgy (reduction) and by thermal decomposition of copper citrate and copper formate.[†] The main stages of synthesis by the reduction method are sedimentation of metals hydroxides, their drying, reduction, and passivation.[16,17] The thermal decomposition of salts was performed in the same reactor *in vacuo*.[18]

[†] The copper hydroxide was synthesized *via* the heterophaseous interaction of $CuCl_2$ and alkali solution upon the limiting dissolution of solid salt. After sedimentation the precipitate was washed out in a Buchner funnel using water to reach pH 7 and then dried in air to obtain dust. A quartz trough with copper hydroxide powder was inserted into the quartz reactor described elsewhere,[16] which was incubated in the furnace at 80 °C in hydrogen flow for 1 h. Then the reactor was taken out from the furnace, cooled to 20 °C in argon flow and placed on the sample platform for video recording. After that, the trough was extracted out of the reactor and placed near it; if necessary, it was blown round with an air fan. In the separate experiments, Cu nanopowder was passivated in the stream of argon and 0.6 vol% O_2 for 30 min and then the trough was extracted out of the reactor.

Upon the thermal decomposition of copper citrate (at 350 °C) and copper formate (at 250 °C) under continuous pumping using both fore vacuum and diffusion pumps, there was an increase in pressure from 10^{-4} to 10^{-1} Torr, the decomposition was considered complete when the residual pressure in the reactor had fallen to less than 10^{-2} Torr. Then the reactor was withdrawn out of the heater and cooled to 20 °C under pumping, only then the quartz trough with Cu nanopowder was placed on the sample platform for high-speed video recording. The withdrawal of the trough and placing it on the platform took about 5 s.

A color high-speed video camera Casio Exilim F1 PRO (60–1200 fps) and the infrared (IR) camera Flir 60 (60 fps, 320×240 pix, sensitivity interval 8–14 μm) were used to establish the modes of combustion of Cu nanopowder. The thickness of the samples was 2 mm. The recording rate was 60 frames per second.

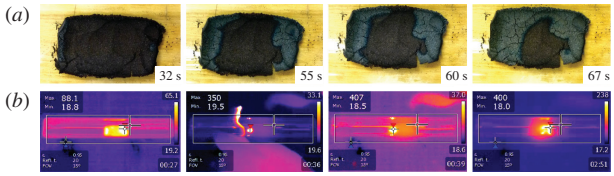

Figure 1 Combustion in the air of Cu nanopowder obtained by chemical metallurgy method: (*a*) self-ignition at 20 °C (the fan is turned on; the time after extraction of the trough with nanopowder from the reactor is shown in the bottom of each frame); (*b*) IR video investigation of the temperature distribution in maximum of warming-up started from 20 °C (the left frame, the fan is turned off) and the ignition initiated by a heated wire [the three frames on the right; the front propagates from the left to the right; the time (min : s) after initiation is shown in each frame].

Self-ignition and combustion in the air atmosphere for Cu nanopowder obtained by chemical metallurgy method is shown in Figure 1(*a*). The velocity of the reaction front estimated as mean velocity of three different points of the front was 0.3±0.02 mm s^{-1}. In Figure 1(*b*), IR investigation of initiated combustion of the same sample, without blowing, is presented.

Upon visual data analysis of IR video filming it is necessary to consider the features of image processing by the Flir 60 infrared camera: the area with the maximum value of temperature has similar brightness for all frames regardless of time from the start of recording. Real values of the maximum and minimum of temperature are shown near the left boundary of each frame. A bigger cross on an each frame specifies the selected point, in which the temperature is taken; the smaller cross automatically specifies a point with maximum of temperature in a frame. On the left frame of Figure 1(*b*), the temperature distribution on a sample surface at the moment of the maximum self-heating (88 °C) is shown (the fan is turned off). This local warming-up at a center of a sample did not lead to propagation of the flame front, and, after being cooled, the sample of Cu nanopowder was ignited with a heated wire [three following frames in Figure 1(*b*)]. Note that the maximal temperature of combustion under these conditions reaches 407 °C, the velocity of the reaction front is 0.3±0.04 mm s^{-1} and agrees with the experiment shown in Figure 1(*a*). Thus, if the trough is blown around, the air fairly reaches the powder and self-ignition occurs properly. In the absence of blowing, the residual Ar flow from the reactor reduces the air flow from the atmosphere to the sample, which is located next to the reactor. Therefore, the self-ignition did not spread. Since such a little change in the experimental conditions leads to a qualitative changes of the modes of interaction between Cu nanopowder and air, Cu nanopowder is obviously highly sensitive to experimental conditions, and that fact correlates well with the results obtained previously.[18] BET surface areas for Cu nanopowder before combustion and Cu nanopowder passivated for 30 min were determined as 13±2 and 10±2 m^2 g^{-1}, respectively. Therefore, the passivation in the stream of mixture of 0.6 vol% O_2 and Ar does not lead to a qualitative change in the value of specific surface of Cu nanopowder.

According to Figure 2(*a*), the surface combustion originally occurs, and the bulk of the nanopowder sample obtained by chemical reduction remains combustible. Indeed, if one extracts the powder from under the oxide layer, the powder ignites (see frames at 182 s, 259 s). The velocity of the combustion front of

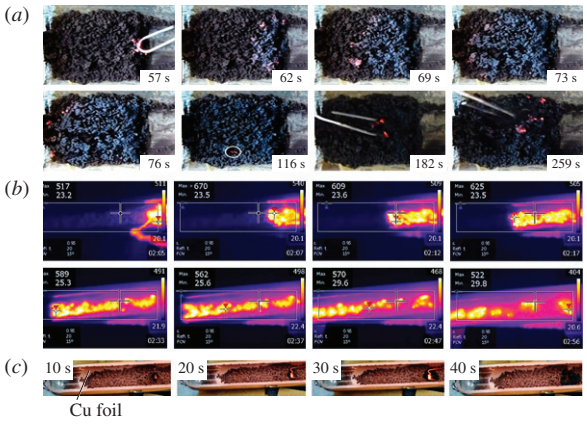

Figure 2 The combustion initiated with a heated wire in air for Cu nanopowders obtained (*a*) from copper citrate at 350 °C (high-speed video recording frames, the time after withdrawal of the trough out of the reactor is shown), (*b*) from copper citrate at 350 °C, IR video recording frames [the time (min : s) after withdrawal of the trough out of the reactor is shown], (*c*) from copper formate at 250 °C, high-speed video recording frames (the time after withdrawal of the trough out of the reactor is shown).

Cu nanopowder obtained from copper citrate was 1.3±0.3 mm s^{-1} and the BET surface area was determined as 45±5 m^2 g^{-1}. Despite the high value of specific surface, we did not manage to obtain self-ignition of the sample even if it was pumped out after synthesis to less than 5×10^{-5} Torr. It is inconsistent with published data,[18] where the Cu powder sample obtained by decomposition of copper citrate and pumped out to 10^{-3} Torr self-ignited in air.

As relating to Figure 2(*b*), the surface combustion originally occurs, and the bulk of the nanopowder ignites when the surface combustion front has already passed. This is evident as the high temperature in that area of the sample, where the combustion front has passed, is stable for tens of seconds (frames 2.47, 2.56) and the temperature maximum shifts from the left end of a sample to its central part. The maximal temperature in the front reaches 625 °C. As follows from the results, *viz.*, increase in specific surface, flame front velocity, and maximal temperature of combustion, one can expect that Cu nanopowder obtained from copper citrate should be pyrophoric. However, Cu nanopowder prepared from copper citrate does not self-ignite, *i.e.*, initially is not pyrophoric. The stability of the powder may be due to its poisoning with CO, which forms during copper citrate decomposition.[19]

In accordance with Figure 2(*c*), copper foil originates during the reaction along with the powder. The Cu nanopowder contains comparably large crystallites, which may be ignited with a heated wire, but its combustion eventually fades. The above results allow one to conclude that thermal decomposition of copper formate is not a perspective way to obtain Cu nanopowder.

Initially, copper formate crystals are quite large [Figure 3(*a*)], and originating copper keeps a form of crystals – precursors [Figures 3(*b*),(*c*), left pictures], while the intermediate substance of decomposition of copper citrate is much less in size (right pictures). In addition, Cu crystallites obtained from copper formate have the morphology of stacked sheets. It allows one to assume that a part of these sheets in further forms a foil, and the remained copper keeps a form of crystallites. As a result, the crystal structure of the initial formate interferes with the formation of nanopowder. This assumption requires further consideration.

Figure 4 shows the SEM photographs of Cu nanopowders. As one can see in Figure 4(*a*), the sample consists of sintered agglomerates. There are particles of 100–200 μm, and less than 20 μm in size. However, all of them represent the sintered agglomerates of smaller particles. The sample presented in Figures 4(*b*),(*c*) is uniform in the size of particles, which is about 10–30 μm. These

Phase composition of the obtained samples was studied by means of a DRON 3M X-ray diffractometer with a coordinate-sensitive detector. The measurement of the values of specific surface was performed *via* BET method using a Sorbi-M analyzer. The microstructure of the powders was examined with a Zeiss Ultra Plus field emission ultra-high resolution scanning electron microscope equipped with an INCA 350 X-ray microanalysis console (Oxford Instruments).

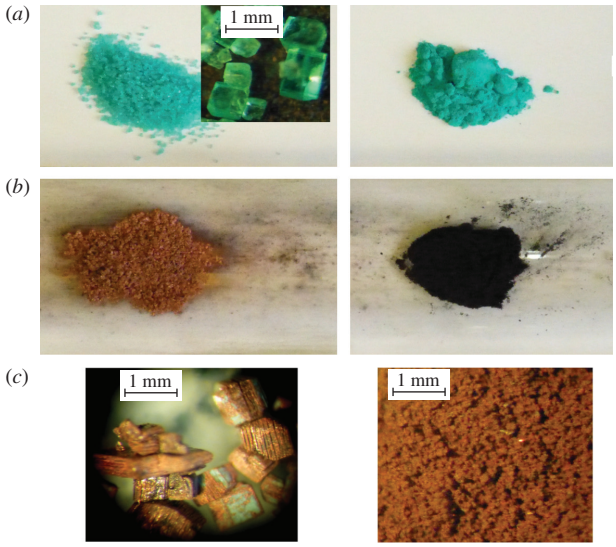

Figure 3 The synthesis of Cu nanopowder *via* decomposition of copper formate (on the left), and copper citrate (on the right): (*a*) initial crystalline precursors; (*b*) intermediate substances after 1 h at 150 °C and 1 h at 200 °C, respectively; (*c*) enlarged fragments of Figure 1(*b*).

particles represent porous agglomerates about 100 nm in size which are visible in the photo as 'binding glue' between particles of a matrix [Figure 4(*c*)]. The hierarchy of structure is well traced, the species of less than 100 nm in size stick together in lamellar structures of 1–2 μm in size, which in turn form separate agglomerated particles of 10–30 μm in size (not shown in Figure 4). The particles of less than 10 nm in size are also observed on the species of less than 100 nm, but due to sintering, it is not quite clear whether the latter consist of 10 nm ones or simply 10 nm particles cover 100 nm ones.

According to the X-ray phase analysis, non-passivated Cu nanopowders obtained *via* different techniques give the similar X-ray spectra (Figure 5). Whereas passivated Cu nanopowder obtained by chemical metallurgy method incorporates noticeable amounts of Cu_2O and CuO, nanopowder obtained from copper citrate contains only CuO traces, *i.e.* the thermal decomposition provides the purer nanopowder.

In conclusion, Cu nanopowders have been synthesized by both a hydrogen reduction (chemical metallurgy) method and thermal decomposition of copper citrate and formate. It was revealed that Cu nanopowder synthesized from copper citrate was not pyrophoric. Its combustion may be initiated by an external source; the velocity of combustion wave was 1.3±0.3 mm s^{-1}. This nanopowder

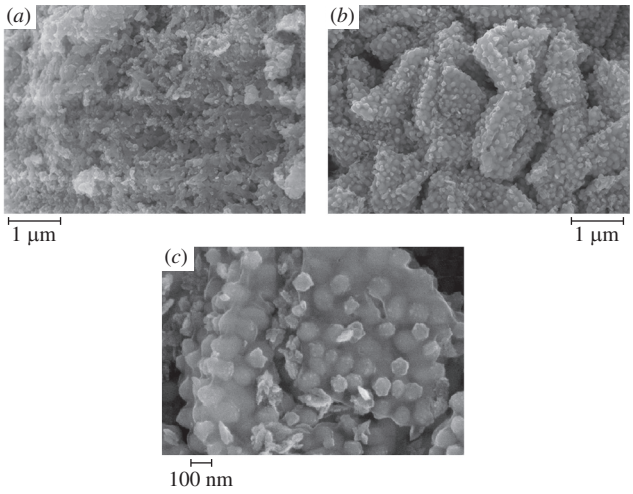

Figure 4 Microphotographs of Cu nanopowders obtained by (*a*) chemical reduction and (*b*), (*c*) thermal decomposition of copper citrate.

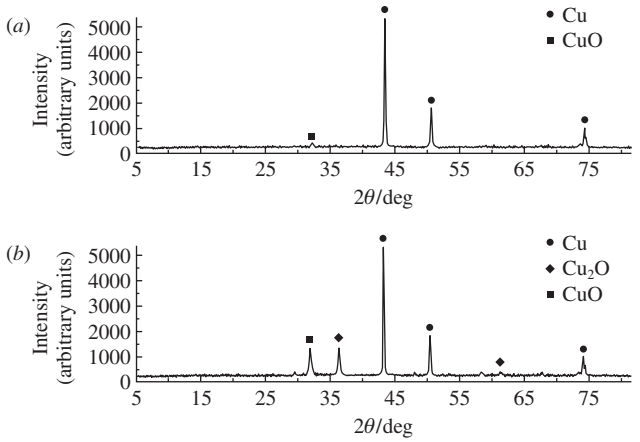

Figure 5 X-ray patterns for Cu nanopowders obtained (*a*) from copper citrate, (*b*) by chemical metallurgy method.

has a specific surface greater by a factor of four (~45±5 m^2 g^{-1}), it does not practically contain oxides and it is stable in air. Cu nanopowder obtained by the chemical metallurgy method is pyrophoric, however, its passivation leads to formation of noticeable amounts of copper oxides. Combustion velocities of the passivated and non-passivated Cu nanopowders are almost equal (0.3±0.04 mm s^{-1}). Dynamics of temperature fields at ignition and combustion of Cu nanopowders produced by various methods has been ascertained.

This work was supported by the Russian Science Foundation (project no. 16-13-00013).

References

1 A. A. Shesterkina, E. V. Shuvalova, E. A. Redina, O. A. Kirichenko, O. P. Tkachenko, I. V. Mishin and L. M. Kustov, *Mendeleev Commun.*, 2017, **27**, 512.
2 A. Kamyshny, J. Steinke and S. Magdassi, *Open Appl. Phys. J.*, 2011, **4**, 19.
3 R. Gréget, G. L. Nealon, B. Vileno, P. Turek, C. Mény, F. Ott, A. Derory, E. Voirin, E. Rivière, A. Rogalev, F. Wilhelm, L. Joly, W. Knafo, G. Ballon, E. Terazzi, J.-P. Kappler, B. Donnio and J.-L. Gallani, *ChemPhysChem*, 2012, **13**, 3092.
4 R. R. Letfullin, C. B. Iversen and T. F. George, *Nanomed. Nanotech. Biol. Med.*, 2011, **7**, 137.
5 Y. Wei, S. Chen, B. Kowalczyk, S. Huda, T. P. Gray and B. A. Grzybowski, *J. Phys. Chem. C*, 2010, **114**, 15612.
6 J. Ramyadevi, K. Jeyasubramanian, A. Marikani, G. Rajakumar and A. A. Rahuman, *Mater. Lett.*, 2012, **71**, 114.
7 N. A. Dhas, C. P. Raj and A. Gedanken, *Chem. Mater.*, 1998, **10**, 1446.
8 H. Hashemipour, M. E. Zadeh, R. Pourakbari and P. Rahimi, *Int. J. Phys. Sci.*, 2011, **6**, 4331.
9 M. Salavati-Niasari and F. Davar, *Mater. Lett.*, 2009, **63**, 441.
10 B. K. Park, D. Kim, S. Jeong, J. Moon and J. S. Kim, *Thin Solid Films*, 2007, **515**, 7706.
11 E. M. Egorova and A. A. Revina, *Colloids Surf. A*, 2000, **168**, 87.
12 R. Zhou, X. Wu, X. Hao, F. Zhou, H. Li and W. Rao, *Nucl. Instrum. Methods Phys. Res., Sect. B*, 2008, **266**, 599.
13 J. N. Solanki, R. Sengupta and Z. Murthy, *Solid State Sci.*, 2010, **12**, 1560.
14 P. Dash, *Res. J. Nanosci. Nanotech.*, 2010, **1**, 25.
15 K. Tian, C. Liu, H. Yang and X. Ren, *Colloids Surf. A*, 2012, **397**, 12.
16 M. I. Alymov, N. M. Rubtsov, B. S. Seplyarskii, V. A. Zelensky and A. B. Ankudinov, *Mendeleev Commun.*, 2016, **26**, 452.
17 M. I. Alymov, N. M. Rubtsov, B. S. Seplyarskii, R. A. Kochetkov, V. A. Zelensky and A. B. Ankudinov, *Mendeleev Commun.*, 2017, **27**, 631.
18 T. M. Gorrie, P. W. Kopf and S. Toby, *J. Phys. Chem.*, 1967, **71**, 3842.
19 B. K. Sharma, *Objective Question Bank in Chemistry*, Krishns Prakashan Media, India, 2009.

Received: 14th November 2017; Com. 17/5405